Upper Extremity Biomechanics of Children with Spinal Cord Injury during Wheelchair Mobility*

Alyssa J. Schnorenberg, Brooke A. Slavens, Adam Graf, Joseph Krzak, Lawrence Vogel, and Gerald F. Harris.

Abstract— **While much work is being done evaluating the upper extremity joint dynamics of adult manual wheelchair propulsion, limited work has examined the pediatric population of manual wheelchair users. Our group used a custom pediatric biomechanical model to characterize the upper extremity joint dynamics of 12 children and adolescents with spinal cord injury (SCI) during wheelchair propulsion. Results show that loading appears to agree with that of adult manual wheelchair users, with the highest loading primarily seen at the glenohumeral joint. This is concerning due to the increased time of wheelchair use in the pediatric population and the impact of this loading during developmental years. This research may assist clinicians with improved mobility assessment methods, wheelchair prescription, training, and long-term care of children with orthopaedic disabilities.**

I. Introduction

There are an estimated 273,000 people in the United States (US) with spinal cord injuries (SCIs), with approximately 12,000 new cases each year [1]. SCIs are one of the leading conditions associated with wheelchair usage [2]. In 2010 there were 124,000 wheelchair users in the US under the age of 21, with 67,000 of these under the age of 15 [3]. Manual wheelchair mobility requires the use of the upper body for maneuvering the wheelchair and performing transfers, weight reliefs and activities of daily living. However, the upper extremity (UE) is not intended for this load magnitude or frequency, and these activities commonly lead to the development of pain and pathologies such as: carpal tunnel syndrome, rotator cuff tears, and shoulder impingement [4, 5].

Upper limb pain and pathologies are likely to develop in over 50% of manual wheelchair users with SCI [6, 7] and have been associated with increased loads, particularly at extreme joint excursions [7, 8]. Longer-term wheelchair usage due to pediatric-onset SCI may cause earlier pain and injury onset and reduce or severely limit the independence, function and quality of life of these children.

Biomechanical analysis has been used to evaluate UE demands during manual wheelchair propulsion in adults [5-11]; however, there has been extremely limited work studying the pediatric population [12].

A greater understanding of pediatric joint motion and loading patterns during manual wheelchair propulsion may lead to identification of risk factors contributing to pain and pathologies. This knowledge may lead to the reduction or cessation of pain and pathology development through improved wheelchair prescription, design, training, and long-term care of children with SCI.

This study aims to characterize three-dimensional (3D) joint dynamics during manual wheelchair propulsion of children with SCI, using a custom, pediatric, inverse dynamics model [13]. Additionally, the study will identify significant differences in average peak loading amongst the glenohumeral, elbow, and wrist joints.

II. Methods

A. Subjects

Twelve pediatric and young adult manual wheelchair users with SCI (2 females / 10 males) were recruited for this study and evaluated at Shriners Hospitals for Children – Chicago. The subjects' average age was 13.2 ±5.0 years. The average height was 137 ±30 cm and weight was 42 ±13 kg. IRB approval was obtained and informed assent or consent was signed by the subject and/or their parent.

B. Data Collection

Subject specific measurements were obtained and 27 passive reflective markers were placed on bony anatomical landmarks and technical locations of the subject, including: suprasternal notch, xiphoid process, spinal process C7, acromion, inferior angle, trigonum spinae, scapular spine (halfway between the trigonum spinae and the acromial angle), acromial angle, coracoid process, humerus technical location, olecranon, ulnar and radial styloids, and the third and fifth metacarpals. A SmartWheel (Out-Front, Mesa, AZ) replaced the wheel on the dominant-side of the subject's wheelchair for kinetic data collection.

The subject propelled his/her manual wheelchair along a 15m path at a self-selected speed using a self-selected propulsion pattern (Fig. 1). A 14-camera Vicon MX System captured the 3D marker trajectories at 120 Hz, while the SmartWheel simultaneously collected 3D forces and

*Research supported by the Department of Education NIDRR grant H133E100007 and NIDRR Advanced Rehabilitation Research Training (ARRT) grant H133P080005.

A. J. Schnorenberg, MS is with the Department of Occupational Science and Technology at the University of Wisconsin-Milwaukee (UWM) and the Rehabilitation Research Design and Disability (R_2D_2) Center at UWM in Milwaukee, WI; (e-mail: paulaj@uwm.edu).

B. A. Slavens, PhD. is with the Department of Occupational Science and Technology at UWM and the R_2D_2 Center at UWM in Milwaukee, WI; Shriners Hospitals for Children, Chicago, IL and the Orthopaedic and Rehabilitation Engineering Center (OREC), at Marquette University (MU) and the Medical College of Wisconsin (MCW), Milwaukee, WI (e-mail: slavens@uwm.edu).

A. Graf, MS, J. Krzak, PhD and L. Vogel, MD are with Shriners Hospitals for Children, Chicago, IL.

G. F. Harris, PhD. is with the Department of Biomedical Engineering, MU, Milwaukee, WI; OREC at MU and MCW, Milwaukee, WI; and Shriners Hospitals for Children, Chicago, IL. (e-mail: gerald.harris@marquette.edu)

moments occurring at the hand–hand-rim interface at 240 Hz. Multiple trials were collected, with adequate rest provided to the subject as needed.

Figure 1. Subject preparing to begin motion analyis with the SmartWheel placed on subject's dominant side.

C. Upper Extremity Biomechanical Model

A custom, bilateral, pediatric UE model was applied to the data to determine 3D joint angles, forces and moments [13]. This biomechanical model comprises 11 segments, including: thorax, clavicles, scapulae, upper arms, forearms and hands. The joints of interest are: three degree-of-freedom thorax, wrist, glenohumeral, and acromioclavicular joints; and two-degree-of-freedom sternoclavicular and elbow joints. Coordinate systems follow ISB recommendation [14] and joint angles are determined with the distal segment with respect to the proximal segment. Matlab (MathWorks, Inc., Massachusetts, USA) was used for model development and data processing.

D. Data Processing

Ten stroke cycles per subject were analyzed to produce a subject average. Subject averages were then used to compute the group average. Time series data of the joint forces and moments were all time normalized to percent of the wheelchair stroke cycle. The stroke cycles were separated into two phases (contact and recovery) based on total force applied to the handrim, with the contact phase sub-divided into periods of propulsive contact (propulsion) and non-propulsive contact (initial contact and release) as determined by the moment about the wheel axle [15].

Forces were normalized to percent body weight (% BW) and moments were normalized to percent body weight times height (% BWxH). Peak forces and moments were determined and two sample t-tests were used to compare average peak loading amongst the glenohumeral (GH), elbow, and wrist joints.

III. Results

A. Temporal-Spatial Parameters

The average propulsion speed was 1.23 m/s ± 0.26 m/s. The average contact and recovery phases occurred from 0% - 35.8% stroke cycle and 35.8% - 100% stroke cycle, respectively. Thus the relative transition time between phases occurred on average at 35.8% stroke cycle, with a range of 25% to 45% stroke cycle. Within the contact phase, the initial contact period occurred on average from 0% – 3.6% stroke cycle, and the release period occurred on average from 34.1% – 35.8% stroke cycle. One subject used the single looping over-propulsion (SLOP) pattern, 3 subjects used the double looping over-propulsion (DLOP) pattern, and 3 subjects used the semicircular (SC) pattern, which is recommended in the literature [7, 11]. The remaining 5 subjects used a variety of patterns.

B. Joint Kinetics

Group mean joint forces, and moments (+/- one standard deviation) of the glenohumeral, elbow and wrist joints were characterized over the wheelchair stroke cycle (Figures 2-3). Each joint's mean peak forces and moments were also computed (Figures 4-5).

The GH joint demonstrated the highest average peak forces, with 6.5 % BW in the posterior direction and 6.1 % BW in the superior direction, which were significantly higher ($p<0.001$) than the posteriorly and superiorly directed forces at the elbow and wrist joints. The highest average joint moment was 1.36% BWxH of elbow flexion, with the GH joint flexion moment significantly less than both the elbow and wrist joint flexion moments ($p<0.01$). The highest average peak GH joint moment was 1.2% BWxH of extension, which was significantly higher than the average peak extension moment of the elbow and wrist joints ($p<0.01$).

IV. Discussion

The average relative time spent in the contact phase of the stroke cycle (35.8%) falls within the range commonly reported for adult manual wheelchair users, which is 30% to 50% [16]. It has been shown that increased relative time of the contact phase is indicative of more challenging tasks, [16]. While the propulsion performed here was not considered challenging by the investigators, a few subjects displayed a relative contact phase time around 45%. Additionally, there were a couple children whose relative time in contact phase was around 25%, slightly below the commonly reported range. Additionally, the model captured times of non-propulsive moments on the handrim, indicating a braking effect, or non-efficient movements. Further, despite the recommended use of the semi-circular pattern in order to achieve the long, smooth propulsive strokes associated with reduced joint loading and cadence [7], the propulsion patterns used by the pediatric population here were varied, with some subjects switching patterns between trials. All of the parameters discussed here may be indicative of inefficient or inappropriate propulsion techniques, possibly resulting in higher joint demands.

The resulting forces and moments are of concern in the pediatric population since they are comparable to the magnitudes reported in adults [8, 9] with similar shoulder impingement risk factors seen in the high GH joint forces directed superiorly and GH joint moments of internal rotation [8]. These findings support continued quantitative evaluation of joint biomechanics for the prevention of pain and overuse injuries, of which these children may be at risk.

The variations seen amongst subjects may be due to mechanical inefficiency, lack of adequate training, and/or asymmetry. This supports the need for subject specific analyses in the future. Further, while the level of SCI has been shown to impact adult joint biomechanics [17], it was not considered here.

Further investigation is underway to explore muscle forces, and the correlations between joint biomechanics and temporal-spatial parameters, as well as injury levels and time of device usage. This could provide valuable information for pediatric wheelchair prescription and training, and long-term transitional care. Ultimately we hope to reduce or eliminate secondary pain and pathology in manual wheelchair users with pediatric-onset SCIs.

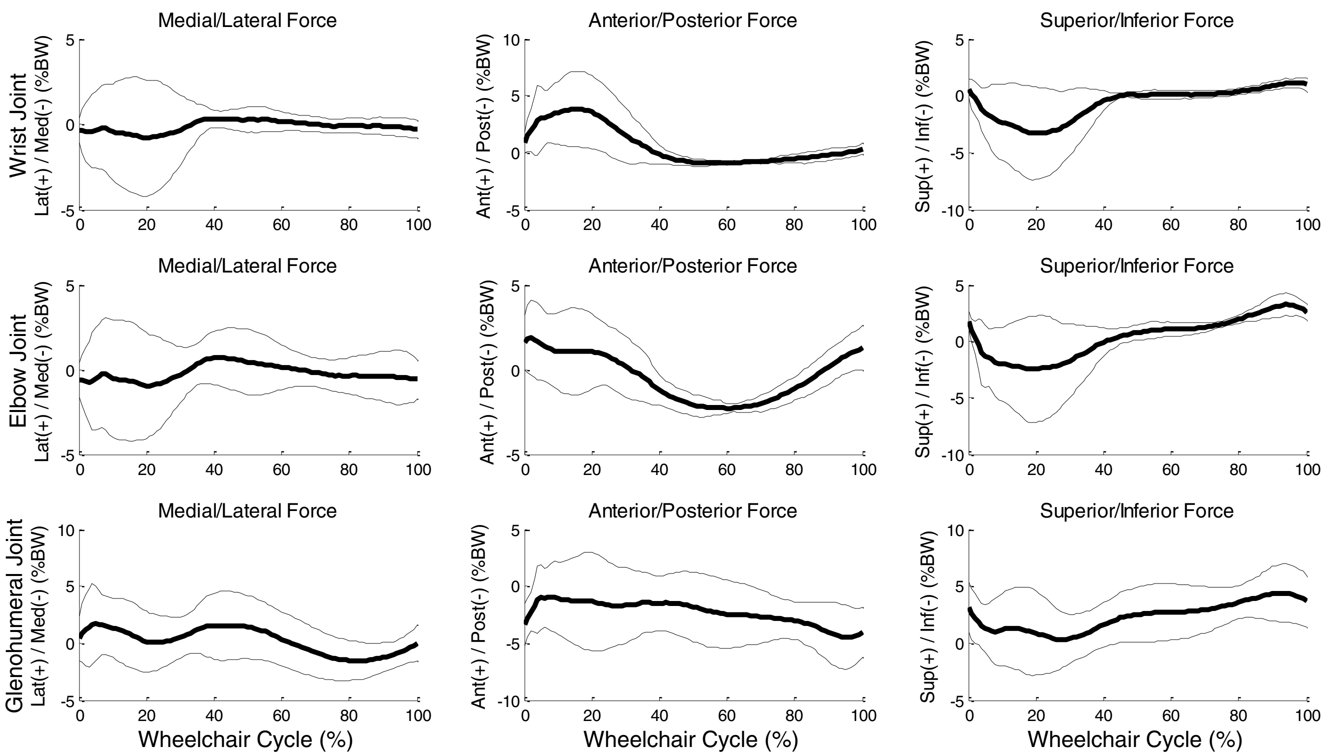

Figure 2. Mean (**bold**) and +/- 1 SD wrist (top row), elbow (middle row) and glenohumeral (bottom row) joint forces in the medial/lateral (left column), anterior/posterior (middle column) and superior/inferior (right column) directions.

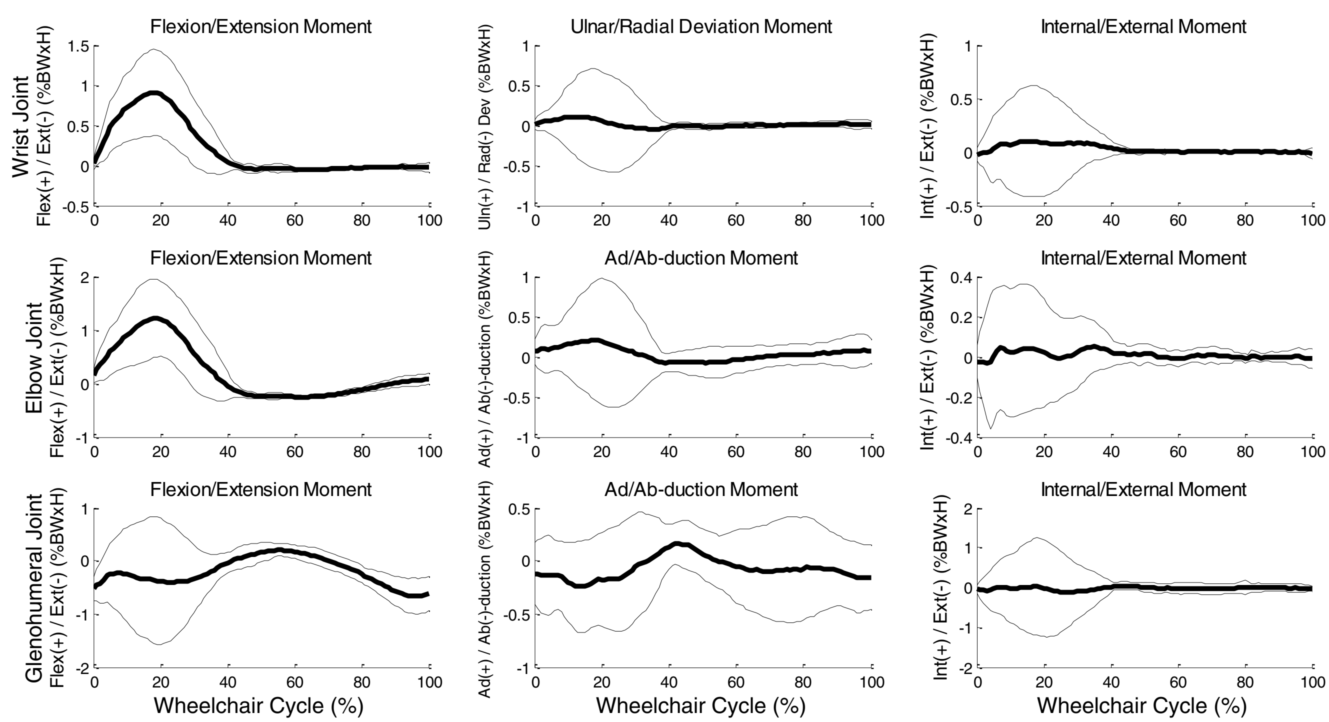

Figure 3. Mean (**bold**) and +/- 1 SD wrist (top row), elbow (middle row) and glenohumeral (bottom row) joint moments in the sagittal (left column), coronal (middle column) and transverse (right column) planes.

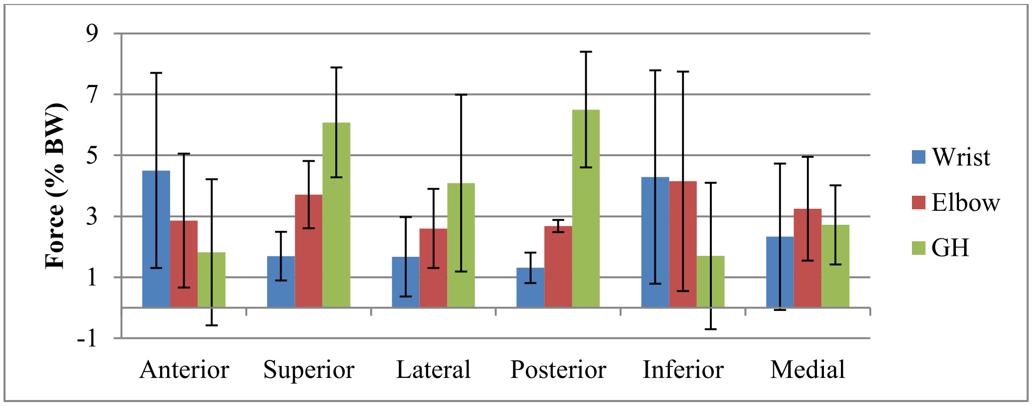

Figure 4. Mean, and standard deviation (bars), peak joint forces in each directcion, for the wrist (blue), elbow (red) and glenohumeral (green) joints.

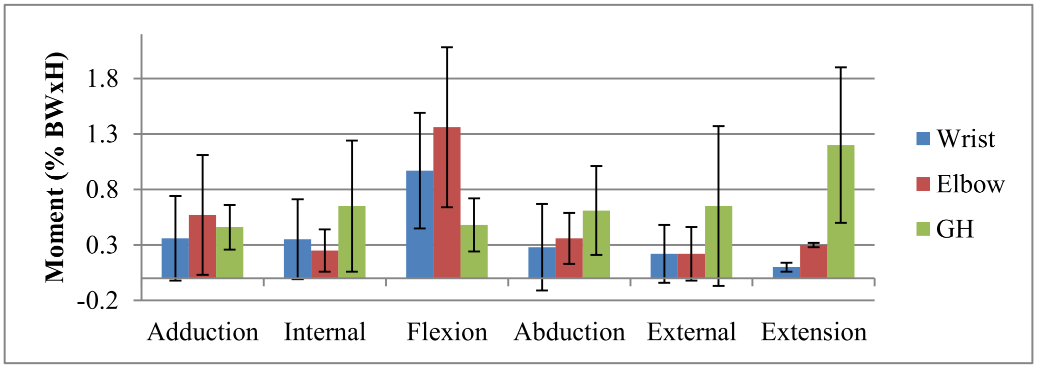

Figure 5. Mean, and standard deviation (bars), peak joint moments for each rotation, for the wrist (blue), elbow (red) and glenohumeral (green) joints.

ACKNOWLEDGMENT

We acknowledge OREC and Shriners Hospitals for Children, Chicago for their support. The contents of this work were developed under a grant from the Department of Education, NIDRR grant number H133E100007. However, the contents of this work do not necessarily represent the policy of the Department of Education, and you should not assume endorsement by the Federal Government. Research reported in this publication was also supported by the Eunice Kennedy Shriver National Institute of Child Health & Human Development of the National Institutes of Health under award number K12HD073945.

REFERENCES

[1] National Spinal Cord Injury Statistical Center, Facts and Figures at a Glance. Birmingham, AL: University of Alabama at Birmingham, March 2013

[2] H. S. Kaye, et al. "Mobility Device Use in the United States," *Disability Statistics Report*, Washington, DC: US Dept Education, NIDRR., vol. 14. pp. 1-60, 2000.

[3] M. W. Brault, "Americans with disabilities: 2010," Washington, D.C.: U.S. Dept. of Commerce, Economics and Statistics Administration, U.S. Census Bureau, 2012.

[4] B. Crane, In M.M. Lusardi, and C. C.Nielsen, *Orthotics and Prosthetics in Rehabilitation* St. Louis, MS: Saunders Elsevier. Ed. 2nd, pp. 489-516, 2007.

[5] H. E. J. Veeger, et al., "Wrist motion in handrim wheelchair propulsion.," *Journal of rehabilitation research and development*, vol. 35, no. 3, pp. 305-13, 1998.

[6] S-h. Wei, S-L. Huang, C-J. Jian, J-C. Chiu, "Wrist kinematic characterization of wheelchair propulsion in various seating position: implication to wrist pain," Clinical Biomechanics, vol. 18, pp. S46-52, 2003.

[7] M. Boninger, A. Koontz, S. Sisto, T. Dyson-Hudson, M. Chang, R. Price, et al., "Pushrim biomechanics and injury prevention in spinal cord injury: recommendations based on CULP-SCI investigations," J Rehab R& D, vol. 42, pp. 9-19, 2005.

[8] J. L. Mercer, M. Boninger, et al., "Shoulder joint kinetics and pathology in manual wheelchair users," *Clinical Biomechanics (Bristol, Avon)*, vol. 21, no. 8, pp. 781-9, 2006.

[9] M. M. Morrow, W. J. Hurd, K. R. Kaufman, and K. N. An, "Shoulder demands in manual wheelchair users across a spectrum of activities," J Electromyogr Kinesiol, vol. 20, pp. 61-7, 2010.

[10] M. M. Morrow, K. R. Kaufman, and K. N. An, "Scapula kinematics and associated impingement risk in manual wheelchair users during propulsion and a weight relief lift," Clinical Biomechanics, vol. 26, pp. 352-7, 2011.

[11] M. Boninger, A. Souza, R. Cooper, S. Fitzgerald, A. Koontz, and B. Fay, "Propulsion patterns and pushrim biomechanics in manual wheelchair propulsion," Arch Phys Med Rehabil, vol. 83, pp. 718-23, 2002.

[12] J. H. Bednarczyk, and D. J. Sanderson, "Limitations of kinematics in the assessment of wheelchair propulsion in adults and children with spinal cord injury," Physical Therapy, vol. 75, no. 4, pp. 281-9, 1995.

[13] A.J. Schnorenberg, B.A. Slavens, M. Wang, L.C. Vogel, P.A. Smith, G.F. Harris, Biomechanical model for evaluation of pediatric upper extremity joint dynamics during wheelchair mobility. *Journal of Biomechanics*, vol. 47, pp. 269-76, 2014.

[14] G. Wu,et al., "ISB recommendation on definitions of joint coordinate systems of various joints for the reporting of human joint motion--Part II: shoulder, elbow, wrist and hand," *Journal of Biomechanics*, vol. 38, pp. 981-92, 2005

[15] A. M. Kwarciak, S. A. Sisto, M. Yarossi, R. Price, E. Komaroff, and M. L. Boninger, "Redefining the manual wheelchair stroke cycle: identification and impact of nonpropulsive pushrim contact," Arch Phys Med Rehabil, vol. 90, pp. 20-6, 2009.

[16] C-J. Lin, P-C. Lin, F-C. Su, "Biomechanics of wheelchair propulsion," Journal of Mechanics in Medicine and Biology, vol. 9, no. 2, pp. 229-42, 2009.

[17] A. Gil-Agudo, et al., "Upper limb joint kinetics during manual wheelchair propulsion in patients with different levels of spinal cord injury," *Journal of biomechanics*, vol. 43, no. 13, pp. 2508-15, 2010.